Article

Safety of Reinforced Concrete Columns: Effect of Initial Imperfections and Material Deterioration under Emergency Actions

Anatoly Victorovich Alekseytsev * and **Natalia Sergeevna Kurchenko**

Department of Reinforced Concrete and Stone Structures, National Research Moscow State
Civil Engineering University, 26, Yaroslavskoye Shosse, 129337 Moscow, Russia
* Correspondence: alekseytsevav@mgsu.ru

Abstract: The effect of (1) initial imperfections and (2) material degradation of reinforced concrete columns on their safety in emergency situations was investigated. The research was limited to low- and medium-flexibility columns. Numerical modeling and proven regulatory methods of analysis were applied to determine the ultimate bearing capacity, taking into account supplementary dynamic loading by a longitudinal force and a bending moment in case of emergency. The numerical model, describing the column structure, has 3D elements simulating concrete, and rebars simulating reinforcement frames (cages). Imperfections are simulated by (1) the physical loss of elements, (2) unzip of nodal elements, and (3) unzip and further zip using nonlinear elements simulating gaps and cohesion between concrete and reinforcement. Implicit dynamics and an incremental method were employed to make computations. Within the framework of this computational scheme, a nonlinear problem was solved using the Newton–Raphson method with nodal forces convergence. The effect of imperfections, such as geometrical deviations and deterioration of mechanical characteristics, on the bearing capacity of compressed bending elements was identified under emergency actions. Risks of mechanical safety loss were analyzed to find that columns in the frame structures of highly hazardous, technically complex, and unique buildings and structures, subjected to supplementary loading, need an additional safety margin in the range of 3–21%. Rectangular cross-sections of columns are the most effective in terms of the safety criterion.

Keywords: emergency risk; numerical modeling; reinforced concrete structures; columns; finite element analysis; supplementary dynamic loading; geometrical imperfections; physical imperfections; safety

1. Introduction

1.1. Review of the Literature on the Problem of Research

Advanced research in the literature focuses on studying the bearing capacity of compressed elements with different types of imperfections. Imperfections are understood as (1) initial deviations of parameters from design values or (2) those deviations that develop in the process of operation. Initial geometrical imperfections are investigated most frequently. Initial geometrical imperfections predetermine decisions that can be made in respect of the arrangement of frame ties [1], simulated using the Monte Carlo method. A number of works, such as [2,3], address the reliability and stability of columns made of cold-formed thin-walled steel, which can be closed and open. The mutual influence of imperfections and the mechanism of steel failure were investigated. Combined systems, made of steel tubes filled with concrete with imperfections, are used apart from thin-walled steel structures [4]. The strength of such structures is studied using numerical simulation based on a finite element method. Apart from initial geometrical imperfections, the effect of residual welding stresses on strength is considered in this work. Dynamics of a multilayer structure, with a geometrically imperfect longitudinal axis, are considered in [5], where

flexible cohesion of layers is also taken into account. Studies on columns, made of steel pipes filled with concrete, are addressed in [6], where the bearing capacity of such structures is identified in an experiment for the case of geometrical deviations in the thickness of the pipe wall. Research results were verified using ANSYS software, and a 9% deviation from the results of numerical analysis from the experiment was recorded. Works [7,8] are no less important studies on such columns. Here, gaps between concrete and a steel pipe, as well as deviations in pipe bending angles, are considered as initial geometrical imperfections. Geometrical imperfections also have a strong effect on the results of thermal strength analyses [9]. This idea is also shared in [10], where geometrical imperfections arise due to buckling caused by the heating of pipes. Of interest are works that investigate structures that (1) have imperfections and (2) are subjected to ultimate dynamic loading [11,12], as well as structures that fail due to initial geometrical imperfection and corrosion defects [13]. At the same time, sensitivity to the source of corrosion and its influence on the collapse mechanism were analyzed, including the case of the symmetrical location of defects. Article [14] is an important work on stability analysis of corrosion-damaged pipes. Here, such important imperfections as centroid displacement and reduction in the pipe cross-section are taken into account. In addition to bearing structures, imperfections are also taken into account in the design of nodal connections. Thus, work [15] studies the ability to transfer internal forces (axial forces and bending moments) through a bolted connection. The influence of imperfections on the resistance of structures is investigated for the case of combined effects [16]. Simulation of low-speed impacts, proposed by the authors, seems to be important here. It is also important to mention the studies on the bearing capacity, stability, and simulation of geometrical imperfections in cylindrical shells, which have already become classical [17–19]. These works study shells made of different materials, including multilayered composite and reinforced concrete shells. In recent works, aimed at designing structures featuring a higher bearing capacity, imperfections of geometrical parameters of webs in corrugated steel beams as well as prefabricated wall sections with V- and ∑-shaped stiffening ribs are considered [20,21]. A large number of studies demonstrate the importance of considering both initial and secondary (those that emerge in the course of the structure operation) imperfections in reinforced concrete structures as well. For example, works [22–24] investigate the effect of imperfections on reinforced concrete structures, mainly columns, under various types of special effects. They include seismic damage, high-temperature effects, and the state of deformation after a fire. Such effects on structures can be fatal even without imperfections, so the issue under study becomes even more relevant.

The stability of rod structures [25], including the transverse stability of columns, especially flexible columns [26–30], is an independent problem where imperfections can also affect mechanical safety. These works consider both geometrical and material imperfections, in particular, initial cracks and concrete strength defects. When simulating these imperfections, transition is made from actual values to statistically valid equivalent values to enable their further use in analytical techniques. Here, analytical dependencies are constructed to evaluate ultimate forces and moments, taking into account the presence of imperfections and their combinations in the structure. Some authors consider defects affecting the cohesion of reinforcement with concrete as imperfections, in addition to under low-cycle loading conditions and the action of fire [31–33]. The use of flexible reinforced concrete and concrete-filled steel columns in structural systems of buildings, and the effect of initial and secondary imperfections on their mechanical safety, energy dissipation properties, nature of loading, etc., are frequently addressed by contemporary authors [34–36].

Attention is also paid to relatively rarely used structures, for example, pre-stressed CFRP-reinforced steel columns with nonmetallic reinforcement [37], and prefabricated beams with FRP and without cohesion [38].

Initial imperfections are taken into account in the course of studying and designing slab structures, flat frame structures of buildings, and tower structures [39–43]. Degradation of their material characteristics as a result of man-induced and natural loads, and the

deviation of the median surface from the idealized position are modeled. The first steps towards the optimization of structures, taking into account the geometry and location of initial imperfections, are made in [37].

This paper addresses an understudied aspect of the problem of imperfection, related to mechanical damage of reinforced concrete columns with medium flexibility and subjected to emergency actions. For example, this includes dynamic overloading at the mechanical removal of the adjacent column, and the ability to bear the loads associated with the localization of collapse from an explosion. It is understood that in standard conditions of operation, imperfections do not have a considerable effect on the bearing capacity of such columns, but their effect is completely different in the case of emergency actions. If imperfections are not taken into account, a dynamically loaded column can suddenly collapse in the case of an accident, leading to the collapse of the whole building.

1.2. Purpose, Objectives, and Overview of the Research in This Article

The purpose of this article is to enhance the safety of buildings and structures with reinforced concrete frames. Columns are among the key sources of major risks of socio-economic losses in an emergency situation. Columns should prevent the propagation of progressive collapse in emergency situations. However, the analysis of dangers triggered by different types of imperfections requires a 3D analysis for the entire structural system of a building. Even now this is problematic, due to the high computational capacity of such calculations. Therefore, it is necessary to propose acceptable approaches and assumptions, discussed in Section 2.1.1, which would help to adequately simulate emergency loads (Section 2.1.2) and describe the stress–strain state (SSS) of systems, subjected to supplementary loading, to achieve this goal. At the same time, SSS by itself does not allow judging the degree of danger of an element failure, because it does not take into account any subsequent damage triggered by the accident. Therefore, the criterion of relative risk, described in Section 2.1.3, is proposed to evaluate mechanical safety.

Simplified finite element schemes, frequently used in engineering calculations, allow determining the SSS of structures quite accurately. In these schemes, bearing elements are geometrically idealized, and characteristics of materials are deterministic constants. Taking account of imperfections seems problematic for such schemes, so a 3D numerical model, described in Section 2.2, was proposed. Section 3.3 presents generalized final results of numerous calculations and some particular results, explaining peculiarities of columns deformation.

The scientific novelty of this research lies in the algorithm of risk analysis, which enables researchers to quantitatively evaluate the mechanical safety of a design solution for reinforced concrete columns. Versatile initial and secondary geometrical and physical imperfections, emerging in the process of long-term operation, are taken into account. Such an evaluation of a design solution is a practical opportunity to enhance the mechanical safety of entire buildings, taking into account the prevention of failures triggered by deviations from regular modes of operation.

2. Materials and Methods

2.1. Statement of the Research Problem

2.1.1. General Statements and Assumptions

The most frequently used square and rectangular cross-sections of columns are considered in this project. Three-dimensional models of columns under dynamic loads (Figure 1) are analyzed using an implicit scheme of integration. In each case the following items are registered: (1) the value of ultimate load, at which the bearing capacity is no longer guaranteed, as well as (2) possible substantial changes in geometry, interpreted as the local loss of stability caused by damages. For this purpose, geometrical nonlinearity is considered as a means of registering coordinate changes in the deformed system. Three possible positions l_1, l_2, l_3 of initial imperfections (Figure 1a) are set.
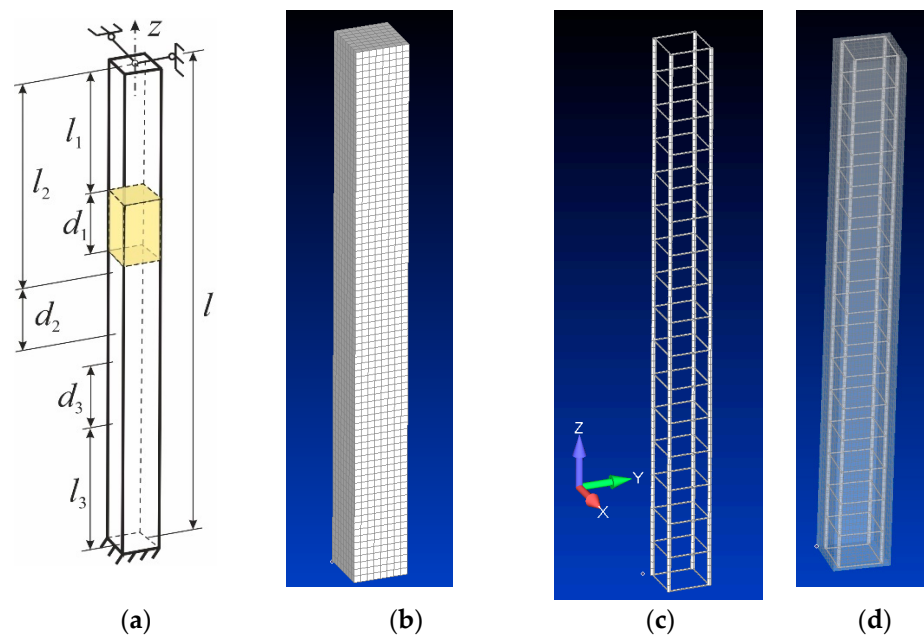
Figure 1. Problem statement: the initial system (**a**) and its representation using the finite element method, simulation of concrete and reinforcement (**b**–**d**): volume, height d_1 as a possible location of an imperfection.

The following items are considered as initial imperfections:

- Deviations in the geometry of rebars from the design position;
- Local buckling of rebars;
- Local failure of the protective layer of concrete accompanied by the loss of cohesion between the reinforcement and concrete;
- Local deterioration of mechanical characteristics of concrete;
- Loss of strength in the connection of reinforcement cage rods as a result of the failure to comply with the welding process requirements.

Symmetrical reinforcement with supplementary vertical loading by the longitudinal force and the bending moment, arising as a result of emergency mechanical damage to the frame structure, was considered when square-section columns were analyzed. In this case, it was assumed that the moment arises in one of the planes perpendicular to the side and passing through the centre of gravity of the section. For rectangular columns, two planes were considered; these were the planes in which the bending moment arose: one plane that was perpendicular to the long side and the other plane that was perpendicular to the short side. The pre-set location of initial imperfections has the maximum effect on the dynamic resistance of a loaded column.

Figure 2 shows cross-sections of columns under consideration, their geometrical parameters and loading patterns, and the computational model. When drafting the computational model, we assumed that the greatest emergency effects were focused on the basement columns, which rigidly rested on the foundation slab. The upper supporting node is considered to be hinged. This assumption is made because, as a rule, a plastic hinge is formed in the junction node connecting the slab and the neighboring loaded column, subjected to supplementary loading in the event of an emergency situation caused by the loss of column. An external moment is applied there (the moment in the plastic hinge in Figure 2a), transmitted by the slab to the column during an emergency situation.
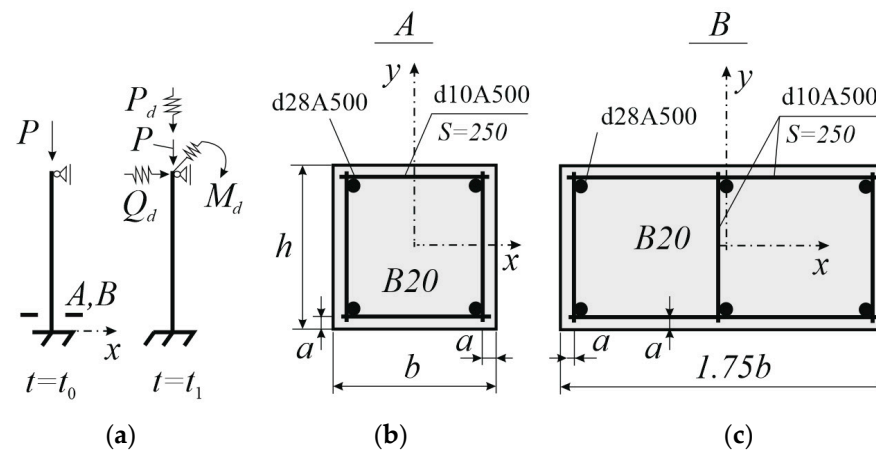
Figure 2. Structural model of the column (**a**), the reinforcement, and types of sections (**b**,**c**).

In Figure 2, the variable t denotes the integration time. At the moment $t = t_0$, the column is under static load, which corresponds to the mode of normal operation. At the moment $t = t_1$, the system is under emergency dynamic overloading. Initial design solutions are based on SP 63.13330 [44], in accordance with which the rebars d28 and d10 (Figure 2b,c) have diameters of 28 and 10 mm, respectively, and the steel grade is A500 (compressive stresses are equal to 420 MPa). Transverse stirrups have a height step of S = 250 mm.

Simulation of an emergency effect on the structural system of a building in the case of its analysis in the 3D formulation requires a substantial amount of computer time. These costs are incomparable with the requirements applicable to the design documentation. Hence, we applied the principle of a degree of detail to a computational model. This principle consists of the fact that a separate structural element is simulated in detail (this is the column we are focused on). The presence of this element in the structural model of a building is simulated by the application of internal forces obtained using an equivalent structural model within the framework of a simplified approach. For example, one can refer to Section 2.1.2 to find the structural model of a frame structure with rod elements (Figure 3).

In the case of emergency dynamic loading, not only the material of reinforced concrete columns can collapse, but columns can lose stability depending on their flexibility. In some works, flexibility values are provided. If the flexibility is $\lambda \geq 50$, material failure is replaced by the loss in stability. In addition to evaluating the flexibility of a square column that we considered, the calculation was carried out to determine the minimum value of the critical force at which the phenomenon of stability loss would be observed. We obtained the value of $P_{ult,b}$, which is more than eight times higher than the real operating load on such a column. Consequently, if the load is higher, the column collapse occurs much earlier than its stability loss. The flexibility of the column is $\lambda_c \approx 22 < 50$. This calculation allows us to not consider the phenomenon of stability loss any further.

2.1.2. Prerequisites for Operational and Supplementary Dynamic Loads

The maximum longitudinal force was evaluated during the period of operation. The value of this force N, applied to the column, is calculated using the formula [45]:

$$N_{ult} = \varphi \times (R_b \times A + R_{sc} \times A_{s,tot}) \tag{1}$$

where R_b is the design resistance of concrete to axial compression; A is the area of concrete section; R_{sc} is the design resistance of the reinforcement to compression; $A_{s,tot}$ is the area of all rebars in the section of the element; and φ is the coefficient of longitudinal bending, depending on the shape of the section and kinematic constraints on the structure.
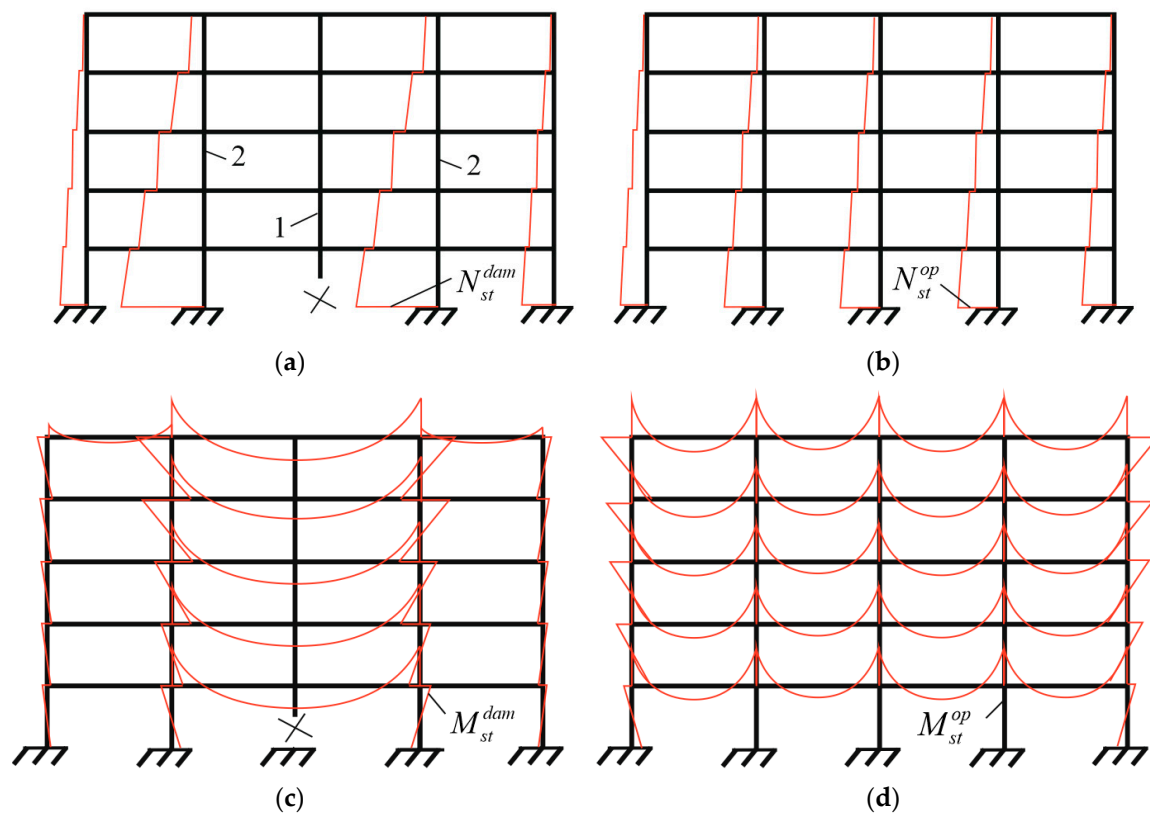
Figure 3. Diagrams of longitudinal forces and moments caused static loading: if the support is removed (1) for forces N (**a**) and M (**c**), the state of normal operation for force N (**b**) and M (**d**) for the nearest column is subjected to supplementary loading (2).

Taking into account the characteristics of concrete class R_b = 14.5 MPa and the reinforcement with the design resistance to compression of 420 MPa, the force value was obtained for a column with a square section of N_{ult} =2750 kN, and for a column with a rectangular section of N_{ult} =4250 kN. To take account of the behavior of a reinforced concrete structure according to recommendations SP 63.13330 [45], the value of the modulus of elasticity of concrete was corrected by factor k_b:

$$k_b = \frac{0.15}{\varphi_l(0.3 + \delta_e)},$$
(2)

where φ_l is the coefficient that takes account of the load action time; δ_e is the relative value of eccentricity of the longitudinal force. In our case study it is $k_b = 0.17$. In turn, the modulus of elasticity of rebars was multiplied by coefficient k_s =0.7.

It is assumed that supplementary dynamic vertical load on the column arises as a result of the local damage to the neighboring column in the frame system. Research, focused on the dynamics of frame structures, shows that the value of the supplementary load depends on many factors, including topology, geometry and parameters of frame elements, nodal connections, and loading intensity. These factors are taken into consideration by applying dynamic coefficient $k_d = 1.15$. The value of the coefficient of supplementary dynamic loading of a column is selected according to the results of the static analysis of the frame, in which the column is located. For a longitudinal force, this coefficient can be found using Figure 3a,b.

$$k_{l(N)} = N_{st}^{dam}/N_{st}^{op},$$
(3)

Then, the following inequality can be made for the limiting value of the longitudinal force in the column, which has no imperfections in the course of operation:

$$N_{st}^{op} = N_d / (k_{l(N)} k_d) \rightarrow N_d / N_{st}^{op} = k_{l(N)} k_d, \tag{4}$$

where N_d is the maximum value of the dynamic force taken by the column before the failure of materials, N_{st}^{op} is the actual value of the longitudinal force in the column during its operation.

Obviously, the supplementary loading coefficient can be determined in terms of bending moments using Formula (3) by substituting N for M only for eccentrically compressed columns. If the column is centrally compressed (conditionally), then the following formula can be used to calculate dynamic moment M_d

$$M_d = k_d M_{st}^{dam} - M_{st}^{op}. \tag{5}$$

Here, M_{st}^{dam} is the moment in the static analysis of an emergency effect (Figure 3c). Formulas (4) and (5) are used to construct functions of a time-driven change in the dynamic load used in Equation (8) of Section 2.2. The value of the horizontal force can be determined as the ratio between the difference of moments at the top and bottom of the column and its geometrical length. For a column with a rectangular cross-section, it is assumed that the dynamic moment acts in the plane of the lowest stiffness of the cross-section.

Verification calculations of dynamic effects were made to justify the consideration of soil base characteristics. The rigid (rock) base and the elastic Winkler base were considered. Calculations show that taking the base into account dampens dynamic effects and reduces the degree of danger of the stress–strain state. Therefore, a decision was made to use the rigid base to most conservatively evaluate the safety of structures.

2.1.3. Mechanical Safety Evaluation Criterion

The criterion for mechanical safety is a structural condition in which the risk of loss of material in an accident is minimized. For clarification purposes, the case of the frame, provided in Figure 3, is considered. It is assumed that if column 2, subjected to supplementary loading, can no longer behave as a bearing structure, then progressive collapse of the entire frame occurs. If it retains its strength, then failure is localized in the two middle spans. In the general case, to evaluate the danger of loss of an element followed by the supplementary loading of the neighboring elements, the value of relative risk is applied:

$$r = \frac{R}{U_{tot}} = \frac{p(\Delta \varepsilon_b) U}{U_{tot}}, \Delta \varepsilon_b = \varepsilon_{ult} - |\varepsilon_b|. \tag{6}$$

where r is the relative risk; R is the absolute risk value; U is the damage caused by the emergency effect during the localization of collapse; U_{tot} is the damage from the complete destruction of the facility; $p(\Delta \varepsilon_b)$ is the probability of failure of the column, subjected to supplementary loading, which can be calculated using the probability theory assuming the normal distribution of random value $\Delta \varepsilon_b$; value ε_{ult} is the greatest value of the main relative deformations of compression; and ε_b is the actual value of such deformations developing during the emergency dynamic loading of the column.

Criterial values of r should be introduced to evaluate mechanical safety. In conditions of uncertainty, the value of $p(\Delta \varepsilon_b)$ will be taken as being equal to 0.5. Let it be assume that safety is considered to be ensured at $r \leq 0.25$. It actually means that in the case of the emergency loss of the column, according to Formula (6), dynamically loaded elements must not lose their strength, and localization of collapse must not exceed 50% of the total damage.

2.2. Dynamic Formulation of the Calculation Method for the Stress–Strain State of Columns with Imperfections

2.2.1. General Equation

Analysis of the stress–strain state of columns is performed using the equation, describing the motion of the system, within the framework of the finite element method, given that columns are subjected to the vertical impact [46]:

$$[M_C + M_R]\ddot{y}(t) + [K_{C\tau} + K_{C\sigma} + K_{R\tau} + K_{R\sigma}](\beta\dot{y}(t) + y(t)) = F(t), \qquad (7)$$

where M_C, M_R are matrices of masses, reduced to nodes, for concrete and reinforcement elements, respectively; $K_{C\tau}$, $K_{R\tau}$ are matrices of minor deformations for concrete and reinforcement elements, respectively; $K_{C\sigma}$, $K_{R\sigma}$ are geometrical matrices for concrete and reinforcement elements, respectively; $\ddot{y}(t)$ is the acceleration vector for time moment t; $\dot{y}(t)$, $y(t)$ are velocity and displacement vectors, respectively; $F(t)$ is the vector of external nodal load, and β is the structural damping factor according to Rayleigh.

2.2.2. Simulation of Imperfections in a Reinforced Concrete Column

The following types of initial imperfections were considered:

- Collapse of a concrete column fragment accompanied by the loss of cohesion between the rebars and concrete (MIM_1);
- Inaccurate design rebar position in the framework (GIM_2);
- Local bending (buckling) of the rebar (GIM_3);
- Defective connection of the cage bars (GIM_4);
- Local deterioration of concrete strength (MIM_4).

Geometrical parameters of imperfections are provided in Table 1.

Table 1. Simulation of the studied imperfections using the case of a square column.
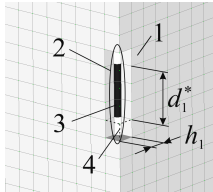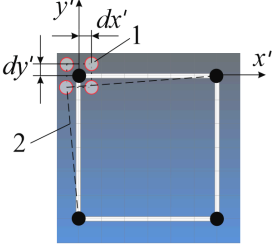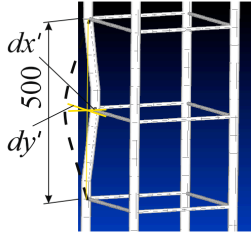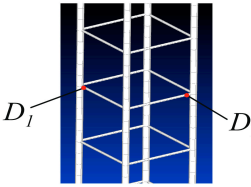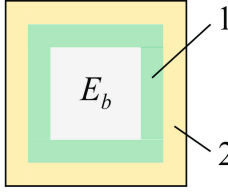
Notation	Location, mm	Size, mm	Model/FE Model	Model Parameters
1	2	3	4	5
MIM_1	$l_1 = 1000$ (Figure 1)	$d_1 = 250$ $d_1^* = 150$	Fragment of a column	$h_1 = 50$ mm; 1—3D FE of concrete; 2—Rod-based FE of reinforcement; 3—FE of reinforcement with the unzip of nodes; 4—Deleted FE of concrete.
	$l_2 = 1750$	$d_2 = 250$ $d_2^* = 150$		
	$l_3 = 1000$	$d_3 = 250$ $d_3^* = 150$		
GIM_2	-	$l = 4000$	Column section	Cases : $dx' = \pm 25$ mm, $dy' = 0$; $dx' = 0, dy' = \pm 25$ mm; $dx' = 25$ mm, $dy' = 25$ mm; $dx' = -25$ mm, $dy' = -25$ mm; 1—possible position of a rod; 2—position of stirrups.

Table 1. *Cont.*

Notation	Location, mm	Size, mm	Model/FE Model	Model Parameters
1	2	3	4	5
GIM_3	$l_1 = 1000$	$d_1 = 500$	Fragment of a frame	Calculation cases : $dx' = 25$ mm, $dy' = 0$; $dx' = 0, dy' = 25$ mm; $dx' = -25$ mm, $dy' = 25$ mm;
	$l_2 = 2000$	$d_2 = 500$		$dx' = 25$ mm, $dy' = 0$; $dx' = 0, dy' = 25$ mm; $dx' = -25$ mm, $dy' = 25$ mm;
	$l_3 = 500$	$d_3 = 500$		$dx' = 25$ mm, $dy' = 0$; $dx' = 0, dy' = 25$ mm; $dx' = -25$ mm, $dy' = 25$ mm;
GIM_4	$l_1 = 1000$	-	Fragment of a frame	Setting the modulus of elasticity for D rods $E = E_s/10^8$. Calculation cases D_1; $D_1 \wedge D_2$
	$l_2 = 2000$	-		D_1
	$l_3 = 500$	-		D_2
MIM_4	$l_1 = 1000$	$d_1 = 500$	Column section (concrete)	Concrete strength deterioration in the layers that are 100 mm thick is simulated 1—Upper layer: Modulus of elasticity $E_{b1} = 0.85E_b$. Cohesion stresses, including cohesion of constrained concrete by rebars $c_1 = 0.8c$. 2—Inner layer: $E_{b2} = 0.4E_b$, $c_2 = 0.35c$
	$l_2 = 2000$	$d_2 = 500$		
	$l_3 = 500$	$d_3 = 500$		

2.2.3. Load Simulation

A model of time-variable loads was used to study the transient process of supplementary emergency-induced dynamic loading. For this purpose, functions $f(t)$, normalized in terms of the value of static load F, were constructed. Hence, at each point in time F_t the value of the load was calculated as

$$F_t = F \cdot f(t). \tag{8}$$

The type of $f(t)$ functions is presented in Section 3. When modeling in volumetric formulation by elements with only linear degrees of freedom in the nodes, the concentrated moments are represented in the form of a pair of follower forces. It is considered that the dynamic overloading is not instantaneous, but over a finite time period. This time can be taken into account by means of function $f(t)$ or experimental information (if available).

2.2.4. Transient Dynamic Process Time

To substantiate the use of numerical integration in time calculations, experimental data from the research literature were used. The authors of experiments provide different values of time, varying from 0.8 s to 3 s, needed for vibrations of reinforced concrete structures to decay and for the system to stabilize. In the analysis of columns, having initial imperfections, the assumed integration time was 3 s after the onset of an emergency

effect. In numerical calculations, no vibration process was detected in the column during this time.

2.2.5. Models of Materials

Concrete was simulated using hexahedral elements, and their deformation was implemented in accordance with the Drucker–Prager plasticity model. Model setting and verification in terms of compliance of the results with the requirements of regulatory calculation methods SP 63.13330 [45] are provided in Section 3. The following values of model parameters were used: cohesion stress (cohesion between particles) C= 3.3 Mpa. This value takes into account an increase in concrete cohesion due to internal compression triggered by frames made of stirrups. In this case, the value of design tensile strength of concrete is R_{bt} = 0.9 MPa. The internal friction angle is φ = 28°; dilatation angle is φ_D = 26°, and relative stresses σ/R_b= 0.3 are considered as the onset of dilatation. To simulate concrete softening, a bilinear function is used, for which at $\varepsilon_{b1} \leq \varepsilon \leq \varepsilon_{b2}$ stresses $\sigma = R_b$, further at $\varepsilon > \varepsilon_{b2}$ stresses σ decreases linearly until the level of deformations ε_f = 0.006 is reached. Here, values of deformations $\varepsilon_{b1}, \varepsilon_{b2}$ correspond to maximum elastic and plastic compression deformations for concrete, respectively, while ε_f are fictitious deformations that ensure the stability of the process of numerical integration. The reinforcement was simulated using the Prandtl bilinear diagram of the steel behavior, in which the value of design resistance R_s = 420 Mpa was used as yield strength, and elastic relative deformations reached $\varepsilon_{s,el}$ = 0.002038.

2.2.6. Algorithm of the Risk Analysis of Mechanical Safety of a Column with Imperfections

The following main stages are implemented:

- Consideration of options of supplementary dynamic loading of the column in terms of different scenarios of local damages. For example, if we take column 2 in Figure 3, we can see that two scenarios of supplementary emergency loading can be implemented for it. The first scenario involves the loss of column 1, as shown in Figure 3, and the second one is implemented in case of the loss of the edge column;
- Calculation of load values, taking into account dynamic effects that arise when an emergency situation is considered for the structural system as a whole. For this purpose, both quasi-static approaches, described in Section 2.1.2, and direct dynamic methods, combined with the principle of the degree of detail, can be used:
- Selection of the location of one or more initial imperfections, as well as predicting the location of secondary imperfections, for example, potential seats of corrosion and open flame in case of fire, etc.;
- Calculation of the finite element model of a column without imperfections and determination of the limit emergency dynamic load the column can take;
- Calculation of the finite element model of the column with imperfections in their least advantageous combination and determination of the limit emergency dynamic load the column can take;
- Comparison of ultimate load values and deciding on the strength margin if the required value of relative risk is to be taken into account (see Section 2.1.3).

3. Results

3.1. Verification of the Calculation Model

The certified preprocessor "Femap Simcenter" 2021 with the solver "Nastran", module: "Transient Nonlinear Analysis" was used for the calculations. The Drucker–Prager model was verified. Parameters of conventional cohesion and the angle of internal friction for the B25 class concrete prisms, of standard sizes $150 \times 150 \times 600$, were selected using the ultimate load criterion of $N_{ult} = R_b A_b = 326.25$ kN. Results of this calculation for the case of the collapse load of 325 kN are presented in Figure 4, which shows that after the achievement of the stress level of 14.5 MPa, quasi-plastic deformation and subsequent collapse commences. Thus, Figure 4a shows the graph of normal stresses (vertical axis) as a

function of vertical force equal to 1 MN acting on the specimen area with dimensions of 150 × 150 mm. The numbers on the horizontal axis indicate the step of loading. At each step, the pressure consistently increases by the magnitude of the increment determined in the nonlinear analysis. The leftmost point shows the stress in the specimen equal to −2.2 MPa, the force is 0.1 of the nominal value of 1 MN. The far right point shows the failure of the specimen. Prior to this (case 7, P = 0.325 MN), stresses of 14.5 MPa approximately equal to the design resistance of the concrete arise in the specimen.
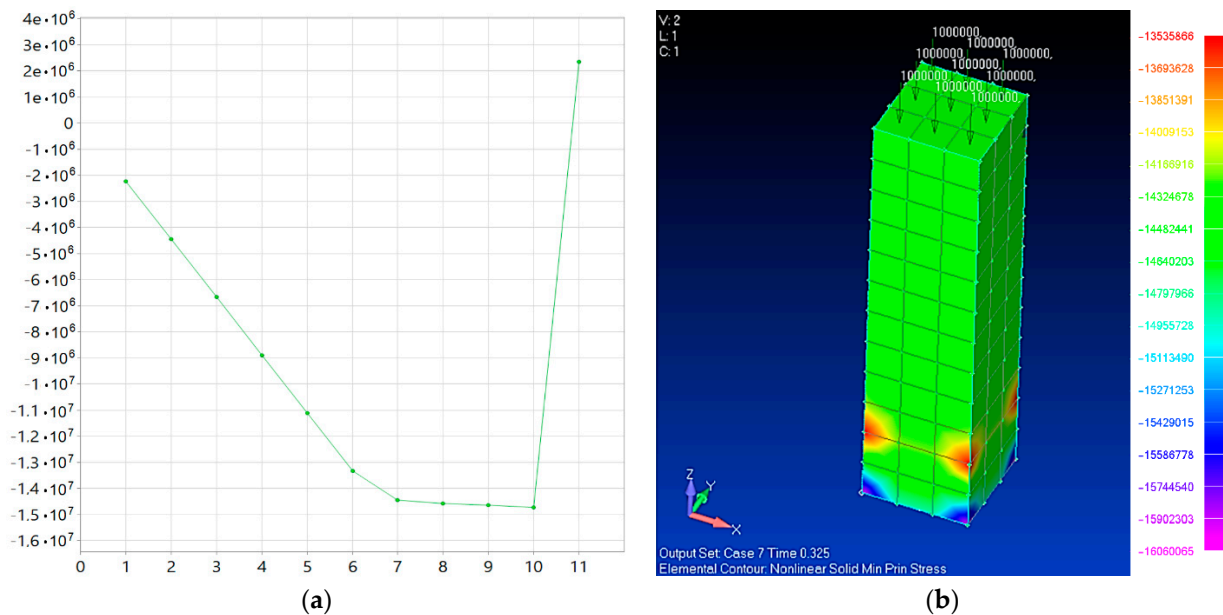

Figure 4. Compression of a standard prism using the Drucker–Prager model, a numerical experiment. Dependence of compressive stresses on dimensionless parametric load (**a**); a prism model with the visualization of the minimum principal stress (**b**).

Further, values of cohesion stresses and the angle of internal friction were selected with allowance for the cohesion of constrained concrete due to the presence of stirrups. The main determinative factor was the bearing capacity, calculated using Formula (1). As a result, concrete characteristics, described in Section 2.2.5, were obtained.

The effect of confinement for concrete is not fully accounted for by approximation for the following reason. The pitch and small diameter of the stirrups, which are significantly deformed in the calculation, are assigned. These strains almost eliminate the constraining effect of the concrete. The presence of the concrete confining was taken into account by increasing the value of cohesion stresses by 10% relative to the unconfined concrete.

3.2. Dynamic Loading and Calculation Parameters

To ensure the precise calculation of coefficients of dynamics, consider the frame structure, shown in Figure 4. The structure has the following parameters.

The total span of the frame is 24 m (6 × 4), the floor height is 3 m. Each floor of the frame is loaded with a uniformly distributed load, with the intensity of 10 kN/m. Columns have dimensions 40 × 40 cm, 40 × 70 cm, girders—40 × 80 (h). Values of internal forces, shown in Table 2, were obtained as a result of the nonlinear static calculations made for the regular conditions of operation at the onset of emergency exposure.

Table 2. Internal forces and calculation of dynamic effects.

№	N_{st}^{dam}, kN	N_{st}^{op}, kN	M_{st}^{dam}, kNm	M_{st}^{op}, kNm	Q_{st}^{dam}, kN	Q_{st}^{op}, kN
1 (40 × 40)	978.6	610.4	35.3	0.5	17.7	0.2
	$N_d/N_{st}^{op} = 1.84$ *		$M_d = 40.09$ **		$Q_d = 20.15$	
2 (40 × 70)	985.5	639.4	75.4	0.9	38.4	0.6
	$N_d/N_{st}^{op} = 1.77$		$M_d = 85.81$		$Q_d = 43.56$	

* Obtained using (4): 1.15 × 978.6/610.4; ** Obtained using Formula (5): 1.15 × 35.3 − 0.5 = 40.09.

Graphs of time functions for the longitudinal force are shown in Figure 5a, for the pair of forces, simulating the effect of the moment—in Figure 5b, and for the transverse force—in Figure 5c. According to Formula (5) and Table 2, the longitudinal force value of F = N = 610.400 kN was introduced in the calculation, for moment F = M/0.3 = 10/0.3 = 33.3333 kN, where 0.3 m is the distance between gravity centers of rebars (see Figure 2b; a = 5 cm), and for transverse force F = Q = 10,000 N. It was assumed that supplementary dynamic loading by the moment and the transverse force takes place within 0.4 s and lags by 0.2 s. Here, complete supplementary loading of the system is achieved at the time moment of t =1.5 s.
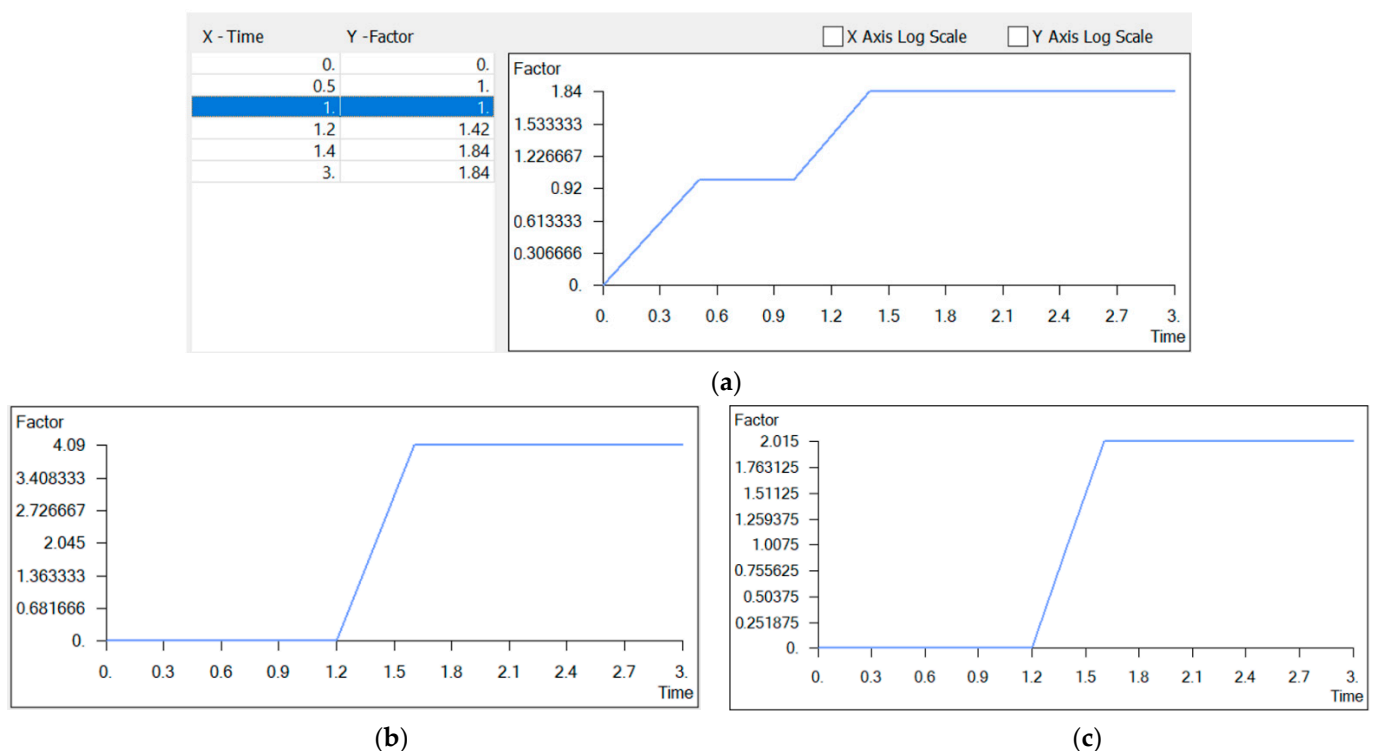
Figure 5. Time functions for modeling the supplementary loading by the longitudinal force (**a**), bending moment (**b**), and transverse force (**c**).

For the purpose of solving the nonlinear problem, using the Newton–Raphson method, it is assumed that parameters of the dynamic calculation include the value of the force convergence error, equal to 0.001. The structural failure criterion is the absence of good conditioning of the system stiffness matrix, accompanied by interruption of the process of numerical integration. An implicit solver ("Femap Simcenter" 2021) is used to analyze dynamics.

3.3. Diagrams of Temporal Variations in SSS Components for Square and Rectangular Columns, Loaded as a Result of Emergency Effects in the Presence and Absence of Imperfections

A number of calculations of finite element models allowed obtaining initial data used for the risk analysis of structures. In fact, in all calculations, rebars of columns reached the yield strength under dynamic loading and thereafter, plastic deformations developed. In a number of calculations the defining role of stirrups was identified. They ruptured due to welding defects in the neighboring rods. The rupture was evaluated by the level of relative strains, which exceeded the limit strain values. Some results of the finite element analysis are shown in Figure 6. Figure 6a,b show that in case of deterioration of mechanical characteristics of concrete surface layers in the bearing part of undamaged concrete, stresses become equal to the design resistance. If the column is insufficiently massive, this can lead to its failure under such supplementary dynamic loading.
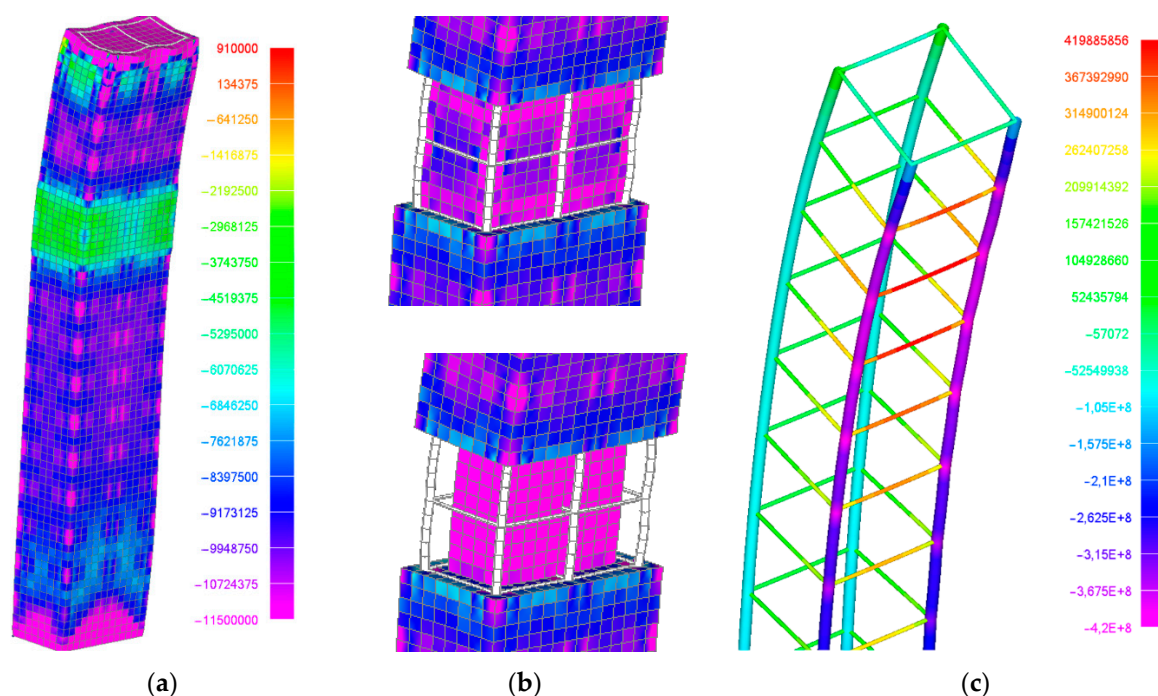

| (**a**) | (**b**) | (**c**) |

Figure 6. Stresses (Pa) in concrete and reinforcement for columns: (**a**) main compressive stresses for the concrete of a rectangular column in the presence of imperfection MIM 4 (location l1); (**b**) visualization of stresses in the internal layers of concrete; (**c**) von Mises stresses (Pa) in the reinforcement cage for a rectangular column without imperfections.

As shown in Figure 6c, stress in stirrups is almost equal to the yield strength under supplementary dynamic loading, which makes welding defects a dangerous imperfection.

3.4. Calculation Results of the Ultimate Dynamic Load in the Presence and Absence of Imperfections

As a result of the initial calculation, the limit value of the longitudinal force was found that corresponded to supplementary dynamic loading of columns without imperfections. For a square column, this value is $N_{ult}^{op} = 1450$ kN in the operating condition; for a rectangular column, it is $N_{ult}^{op} = 2260$ kN. Results of further calculations show that structural failure is observed under such loading and in the presence of some imperfections. In this regard, it seems reasonable to determine the load at which the presence of imperfections does not have a major effect on the bearing capacity. A search was performed with a 25 kN decrease in the value of the ultimate longitudinal force. It is found that for a square column, the value of SSS, at which the effect of imperfections on the bearing capacity is insignificant, is close to the limit value and equal to $N_{st,imp}^{op} = 1400$ kN; for a rectangular

column it is $N_{ult}^{op} = 2210$ kN. The data on the condition of columns under supplementary dynamic loading and the presence of imperfections of different types are presented in Table 3. Imperfections are titled according to Table 1.

Table 3. Results of the column calculation, taking into account imperfections.

№	Calculation of Columns With Imperfections	Loading Value Used for Dynamic Calculation Purposes			
		Square Section Column		Rectangular Section Column	
		$N_{st}^{op} = 1450$ kN $M_d = 40.09$ kNm	$N_{st,imp}^{op} = 1400$ kN $M_d = 40.09$ kNm	$N_{st}^{op} = 2260$ kN $M_d = 85.81$ kNm	$N_{st}^{op} = 2210$ kN $M_d = 85.81$ kNm
1	2	3	4	5	6
1	GIM_1 (location l_1)	Collapse accompanied by the formation of a geometrically changeable system (mechanism), further collapse $t = 1.512$ s	The bearing capacity is ensured	The bearing capacity is ensured	-
2	GIM_1 (location l_2)	Collapse $t = 1.524$ s	The same (-//-)	The same (-//-)	-
3	GIM_1 (location l_3)	Collapse $t = 1.580$ s	-//-	-//-	-
4	GIM_2 (displacement towards the face that is parallel to the plane of action of the moment) $dx' = -25, dy' = 0;$	Collapse $t = 1.570$ s	-//-	Collapse $t = 1.512$ s	The bearing capacity is ensured
5	GIM_2 (displacement from the face that is parallel to the plane of action of the moment) $dx' = 25, dy' = 0;$	The bearing capacity is ensured	-//-	The bearing capacity is ensured	-
6	GIM_2 (inward displacement) $dx' = 25, dy' = -25;$	The bearing capacity is ensured	-//-	The bearing capacity is ensured	-
7	GIM_2 (displacement towards faces) $dx' = -25, dy' = 25;$	Collapse $t = 1.570$ s	-//-	Collapse $t = 1.482$ s	The bearing capacity is ensured
8	GIM_3 (location l_1) $dx' = 25, dy' = 0;$	Collapse $t = 1.542$ s	-//-	Collapse $t = 1.540$ s	The bearing capacity is ensured
9	GIM_3 (location l_2) $dx' = 25, dy' = 0;$	The bearing capacity is ensured	-//-	The bearing capacity is ensured	-
10	GIM_3 (location l_3) $dx' = 25, dy' = 0;$	Collapse $t = 1.521$ s	-//-	The same	-
11	GIM_3 (location l_1) $dx' = 0, dy' = 25;$	The bearing capacity is ensured	-//-	-//-	-

Table 3. *Cont.*

№	Calculation of Columns With Imperfections	Loading Value Used for Dynamic Calculation Purposes			
		Square Section Column		Rectangular Section Column	
		N_{st}^{op} = 1450 kN M_d = 40.09 kNm	$N_{st,imp}^{op}$ = 1400 kN M_d = 40.09 kNm	N_{st}^{op} = 2260 kN M_d = 85.81 kNm	N_{st}^{op} = 2210 kN M_d = 85.81 kNm
1	2	3	4	5	6
12	GIM_3 (location l_2) $dx' = 0, dy' = 25$;	The same	-//-	-//-	-
13	GIM_3 (location l_3) $dx' = 0, dy' = 25$;	Collapse $t = 1.542$ s	The bearing capacity is ensured	The bearing capacity is ensured	-
14	GIM_3 (location l_1) $dx' = -25, dy' = 25$;	Collapse $t = 1.524$ s	The same	Collapse $t = 1.557$ s	The bearing capacity is ensured
15	GIM_3 (location l_2) $dx' = -25, dy' = 25$;	Collapse $t = 1.544$ s	-//-	The bearing capacity is ensured	-
16	GIM_3 (location l_3) $dx' = -25, dy' = 25$;	The bearing capacity is ensured	-//-	The same	-
17	GIM_4 (location l_1) D_1 $D_1 \wedge D_2$	The bearing capacity is ensured	-//-	-//-	-
18		Collapse Collapse$t = 1.517$ s	-//-	Collapse $t = 1.492$ s	The bearing capacity is ensured
19	GIM_4 (location l_2) D_1 $D_1 \wedge D_2$	Collapse $t = 1.52$ s	-//-	The bearing capacity is ensured	-
20		Collapse $t = 1.559$ s Deformations $\varepsilon_s \approx 0.04 \gg 0.015$ (stirrup rupture)	-//-	Collapse $t = 1.562$ s (stirrup rupture) $\varepsilon_s \approx 0.025 \gg 0.015$	The bearing capacity is ensured
21	GIM_4 (location l_3) D_1 $D_1 \wedge D_2$	Collapse $t = 1.518$ s	The bearing capacity is ensured	The bearing capacity is ensured	-
22		Collapse $t = 1.517$ s	The bearing capacity is ensured	Collapse $t = 1.496$ s	The bearing capacity is ensured
23	MIM_4 (location l_1)	Collapse, $t = 1.480$ s (failure in the damage area)	Collapse $t = 1.54$ s The bearing capacity is ensured at $P = 1200$ kN $M_d = 40.09$ kNm	Collapse $t = 1.523$ s	Collapse $t = 1.568$ s The bearing capacity is ensured at $P = 2010$ kN $M_d = 40.09$ kNm
24	MIM_4 (location l_2)	Collapse $t = 1.514$ s	The bearing capacity is ensured	The bearing capacity is ensured	-
25	MIM_4 (location l_3)	Collapse $t = 1.440$ s	The bearing capacity is ensured $\sigma_b = R_b$	Collapse $t = 1.541$ s	The bearing capacity is ensured

3.5. Risk Analysis of Mechanical Safety of Columns with Imperfections

The qualitative analysis of the table shows that the rectangular section is more resistant to failures under emergency effects. Table 4 has a quantitative evaluation made using the data obtained as a result of the finite element calculations.

Table 4. Calculation results of the column, taking into account imperfections.

№	Design	Imperfections Numbered as in Table 2	β_ε	$p(\Delta\varepsilon_b)$,%	r
1	Column section 400 × 400 (h)	1–4, 7, 8, 10, 13–15, 18–25.	1.3608	15.8	0.0158
2	Column section 700 × 400 (h)	4, 7, 8, 14, 18, 20, 22, 23, 25.	1.6954	9.47	0.00947

If Formula (6) is applied, $U/U_{tot} = 0.1$ is used for the frame structure, and the value of $p(\Delta\varepsilon_b)$ is calculated on the basis of the assumption of normal distribution of the random value of deformation margin $\Delta\varepsilon_b$.

This assumption is accepted since in this structure, concrete is the material that better ensures its bearing capacity. The following reliability theory formulas are used to make calculations in the table:

$$\delta(\Delta\varepsilon_b) = \sqrt{S^2(\sigma_1/E_{b0}) + S^2(R_b/E_{b0})}, \tag{9}$$

$$\beta_\varepsilon = \frac{\Delta\bar{\varepsilon}_b}{\delta(\Delta\varepsilon_b)}, \tag{10}$$

$$p(\Delta\varepsilon_b) = 1 - (0.5 + \Phi(\beta_\varepsilon)), \tag{11}$$

where $\Delta\bar{\varepsilon}_b$ is the mathematical expectation of the value $\Delta\varepsilon_b$ taking into account the considered imperfections; $S^2(\sigma_1/E_{b0})$, $S^2(R_b/E_{b0})$ are mean-square deviations of actual and limiting deformations, respectively; and σ_1, E_{b0}, R_b are the main compressive stresses, the initial modulus of elasticity, and the design compressive strength for concrete, respectively. The table includes those calculations in which the condition of the column performance is ensured for the imperfection under consideration. Cells with dashes are disregarded, since the risk of failure is close to zero here.

As a result of the risk analysis carried out in Table 4, it is found that the column with a 700 × 400 mm cross-section is safer under dynamic emergency loads (the risk value is smaller for it). This method also allows for evaluating the level of the relative risk for other bearing structures and normalizing the relative risk.

4. Discussion and Prospects for Further Investigation

The analysis of the table shows that initial geometrical imperfections do not have a great effect on the bearing capacity of columns, if the design has a safety margin, taking into account supplementary dynamic emergency loading. For square and rectangular columns, this margin can vary from 3 to 5%.

Secondary imperfections, caused by man-induced or natural factors deteriorating the mechanical characteristics of materials, have a greater effect. Hence, for the square column under consideration, a safety margin of the bearing capacity of up to 21% is required to ensure trouble-free operation. Rectangular columns are more resistant to such effects and require a safety margin of 13%. If the safety margins are lower under emergency loading, the presence of imperfections can lead to the progressive collapse of the frame system due to the failure of the column subjected to supplementary loading.

Obviously, locations of initial imperfections, their geometry, and topology can be chosen in various combinations and their effect on the bearing capacity can be refined.

This problem can be solved using optimization algorithms of the search type, in which sets of imperfection parameters are used as variable parameters. The maximum load at which the bearing capacity of the column can be ensured, taking into account emergency dynamic loading by vertical load and bending moment, is the purpose of optimization. Calculations and results of risk analysis show that the symmetrical shape of the column cross-section is less sensitive to the presence of imperfections. It is safer at equal load intensities, close to the limit values.

Based on the approach outlined in this work, prospects for further research are related to the following aspects:

- Analysis of mechanical safety of columns with imperfections, and if these columns are subjected to special impacts, including lateral horizontal and angular impacts;
- Improvement in simulation accuracy based on the simulation of the brittle failure of concrete using local GAP elements;
- Risk analysis of safety of columns and other key bearing elements of buildings with advanced reinforcement patterns;
- Development of optimization methods, taking into account the risk analysis for building frameworks, and the formation of algorithms needed to identify the worst combinations of imperfections, for example, those that are based on the algorithms outlined in papers [45,47,48].

5. Conclusions

1. An approach to risk analysis and modeling of columns is proposed. This approach allows obtaining safe design solutions in the presence of initial or secondary imperfections and emergency situations not foreseen in the course of normal operation. This approach is based on the reliability theory and the principle of continuum discretization of the calculation model;
2. In the presence of initial or secondary imperfections and emergence of supplementary emergency dynamic loads, columns with square and rectangular cross-sections and medium and low flexibility (collapsing due to the failure of their material rather than the loss in stability) must be designed with a safety margin of 3–21%;
3. The developed approach to the risk analysis of an emergency situation shows that the smallest risk of column failure is observed for a rectangular cross-section and symmetrical reinforcement.

References

1. Zhao, J.; Wei, J.; Wang, J. Design Forces of Horizontal Braces Unlocated at Middle of Columns Considering Random Initial Geometric Imperfections. *Adv. Civ. Eng.* **2021**, *2021*, 1264270. [CrossRef]
2. Brambatti, N., Jr.; Walber, M.; de Meira, A.D., Jr. Initial Geometric Imperfections: A Robust, Closed-Section Cold-Formed Box Profile Application Subject to Local Buckling. *Int. J. Appl. Mech. Eng.* **2021**, *26*, 18–44. [CrossRef]
3. Harvey, P.S.; Cain, T.M.N. Buckling of Elastic Columns with Initial Imperfections and Load Eccentricity. *Structures* **2020**, *23*, 660–664. [CrossRef]

4. Lu, X.; Liu, Y.-J.; Sun, L.-P.; Jiang, L. Effect of Initial Imperfection on Post-Buckling Strength of Concrete-Filled Rectangular Steel Tubular Column Slab. *J. Archit. Civ. Eng.* **2020**, *37*, 170–181. [CrossRef]
5. Adam, C.; Ladurner, D.; Furtmüller, T. Moderately Large Vibrations of Flexibly Bonded Layered Beams with Initial Imperfections. *Compos. Struct.* **2022**, *299*, 116013. [CrossRef]
6. Ahmad, H.; Fahad, M.; Aslam, M. Nonlinear Numerical Analysis and Proposed Equation for Axial Loading Capacity of Concrete Filled Steel Tube Column with Initial Imperfection. *Struct. Monit. Maint.* **2022**, *9*, 81–105. [CrossRef]
7. Kumar, M.; Roy, P.; Khan, K. Determination of Collapse Moment of Different Angled Pipe Bends with Initial Geometric Imperfection Subjected to In-Plane Bending Moments. *Proc. Inst. Mech. Eng. Part C J. Mech. Eng. Sci.* **2022**, *236*, 525–535. [CrossRef]
8. Yu, P.; Ren, Z.; Yun, W.; Zhao, Y.; Xu, J. Performance of Bolt-Welded CFST Short Columns with Different Initial Imperfections: Experimental and Numerical Studies. *Buildings* **2022**, *12*, 1352. [CrossRef]
9. Cetkovic, M. Influence of Initial Geometrical Imperfections on Thermal Stability of Laminated Composite Plates Using Layerwise Finite Element. *Compos. Struct.* **2022**, *291*, 115547. [CrossRef]
10. Xu, J.-Q.; She, G.-L. Thermal Post-Buckling Analysis of Porous Functionally Graded Pipes with Initial Geometric Imperfection. *Geomech. Eng.* **2022**, *31*, 329–337. [CrossRef]
11. Shi, G.-J.; Wang, D.-Y.; Hu, B.; Cai, S.-J. Effect of Initial Geometric Imperfections on Dynamic Ultimate Strength of Stiffened Plate under Axial Compression for Ship Structures. *Ocean. Eng.* **2022**, *256*, 111448. [CrossRef]
12. Hara, T.; Kato, S.; Gould, P.L. Ultimate Strength of R/C Cooling Tower Shell with Various Reinforcing Ratios. *J. Int. Assoc. Shell Spat. Struct.* **1996**, *37*, 153–162.
13. Zhou, L.; Yuan, L.; Gong, S. On the Collapse of Thick-Walled Steel Pipes under Coupling Initial Geometric Imperfection and Corrosion Defect. *Ships Offshore Struct.* **2022**, *18*, 325–337. [CrossRef]
14. Øyasæter, F.H.; Aeran, A.; Siriwardane, S.C. A Formula for Estimating the Buckling Capacity of Corroded Tubular Members. *Int. J. Struct. Integr.* **2022**, *13*, 951–984. [CrossRef]
15. Gil, B.; Gracia, J.; Bayo, E. Axial-Moment Interaction for 2D Extended End Plate Bolted Steel Connections. Experimental Investigation and Assessment of the Initial Imperfections. *J. Build. Eng.* **2022**, *60*, 105134. [CrossRef]
16. Zhang, W.; Guo, L.-J.; Wang, Y.; Mao, J.-J.; Yan, J. Nonlinear Low-Velocity Impact Response of GRC Beam with Geometric Imperfection under Thermo-Electro-Mechanical Loads. *Nonlinear Dyn.* **2022**, *110*, 3255–3272. [CrossRef]
17. Feng, S.; Duan, Y.; Yao, C.; Yang, H.; Liu, H.; Wang, B.; Hao, P. A Gaussian Process-Driven Worst Realistic Imperfection Method for Cylindrical Shells by Limited Data. *Thin-Walled Struct.* **2022**, *181*, 110130. [CrossRef]
18. Jeon, M.-H.; Cho, H.-J.; Sim, C.-H.; Kim, Y.-J.; Lee, M.-Y.; Kim, I.-G.; Park, J.-S. Experimental and Numerical Approach for Predicting Global Buckling Load of Pressurized Unstiffened Cylindrical Shells Using Vibration Correlation Technique. *Compos. Struct.* **2023**, *305*, 116460. [CrossRef]
19. Elferink, B.; Eigenraam, P.; Hoogenboom, P.C.J.; Rots, J.G. Shape Imperfections of Reinforced Concrete Shell Roofs. *Heron* **2016**, *61*, 177–192.
20. Wang, S.; Zhang, K.; Zhang, Y.; Liu, Y. Shear Failure Mechanism of Local Buckling-Dominated Large-Scale Corrugated Steel Web. *Thin-Walled Struct.* **2023**, *182*, 110279. [CrossRef]
21. He, Z.; Peng, S.; Zhou, X.; Yang, G.; Schafer, B.W. Failure Characteristics of Cold-Formed Steel Built-up Sections with Web Stiffeners under Axial and Eccentric Compression. *Thin-Walled Struct.* **2023**, *182*, 110269. [CrossRef]
22. Kato, M.; Michikoshi, S.; Baba, S.; Sakata, H. Behavior of Slender RC Columns with Initial Deformation in Fire: Study on Fire Resistance of Slender RC Columns Part 2. *J. Struct. Constr. Eng.* **2017**, *82*, 959–968. [CrossRef]
23. Yang, Y.; Gu, X. Collapse Simulation of Damaged Reinforced Concrete Frame Structures in Earthquakes. In *The Evolving Metropolis-Report, Proceedings of the 20th Congress of IABSE, New York, NY, USA, 4–6 September 2019*; International Association for Bridge and Structural Engineering (IABSE): Zurich, Switzerland, 2019; pp. 1012–1017.
24. Mahmoud, K.A. Overview of Factors Affecting the Behavior of Reinforced Concrete Columns with Imperfections at High Temperature. *Fire Technol.* **2022**, *58*, 851–887. [CrossRef]
25. Kolodziejczyk, A.; Höller, T.; Maurer, R.; Sauermann, K. Investigation of Initial Imperfections for the Analysis of Slender Beams against Lateral Instability | Untersuchungen Zum Ansatz Der Vorverformungen Beim Nachweis der Kippsicherheit Schlanker Träger. *Beton- Und Stahlbetonbau* **2016**, *111*, 408–418. [CrossRef]
26. Kalkan, I.; Bocek, M.; Aykac, S. Lateral Stability of Reinforced-Concrete Beams with Initial Imperfections. *Proc. Inst. Civ. Eng. Struct. Build.* **2016**, *169*, 727–740. [CrossRef]
27. Wahrhaftig, A.M.; da Silva, M.A.; Brasil, R.M.L.R.F. Analytical Determination of the Vibration Frequencies and Buckling Loads of Slender Reinforced Concrete Towers. *Lat. Am. J. Solids Struct.* **2019**, *16*, 1–31. [CrossRef]
28. de Macêdo Wahrhaftig, A. Time-Dependent Analysis of Slender, Tapered Reinforced Concrete Columns. *Steel Compos. Struct.* **2020**, *36*, 229–247. [CrossRef]
29. Oh, J.Y.; Lee, D.H.; Lee, J.; Kim, K.S.; Kim, S.-B. Experimental Study on Reinforced Concrete Column Incased in Prefabricated Permanent Thin-Walled Steel Form. *Adv. Mater. Sci. Eng.* **2016**, *2016*, 3806549. [CrossRef]
30. Pissinatti, C.; Poncetti, B.L.; Buchaim, R.; Vanderlei, R.D. The Influence of the Reinforced Concrete Deformability in the Design of Slender Columns. *Eng. Struct.* **2021**, *245*, 112882. [CrossRef]

31. Trujillo, P.B.; Jolin, M.; Massicotte, B.; Bissonnette, B. Bond Strength of Reinforcing Bars Encased with Shotcrete. *Constr. Build. Mater.* **2018**, *169*, 678–688. [CrossRef]
32. Zou, R.; Liu, F.; Xiong, Z.; He, S.; Li, L.; Wei, W. Experimental Study on Fatigue Bond Behaviour between Basalt Fibre-Reinforced Polymer Bars and Recycled Aggregate Concrete. *Constr. Build. Mater.* **2021**, *270*, 121399. [CrossRef]
33. Wang, W.-H.; Han, L.-H.; Tan, Q.-H.; Tao, Z. Tests on the Steel–Concrete Bond Strength in Steel Reinforced Concrete (SRC) Columns After Fire Exposure. *Fire Technol.* **2017**, *53*, 917–945. [CrossRef]
34. Ci, J.; Ahmed, M.; Liang, Q.Q.; Chen, S.; Chen, W.; Sennah, K.; Hamoda, A. Experimental and Numerical Investigations into the Behavior of Circular Concrete-Filled Double Steel Tubular Slender Columns. *Eng. Struct.* **2022**, *267*, 114644. [CrossRef]
35. Yan, B.; Zhou, X.; Liu, J. Behavior of Circular Tubed Steel-Reinforced-Concrete Slender Columns under Eccentric Compression. *J. Constr. Steel Res.* **2019**, *155*, 342–354. [CrossRef]
36. Savin, S.Y.; Kolchunov, V.I. Dynamic behavior of reinforced concrete column under accidental impact. *Int. J. Comput. Civ. Struct. Eng.* **2021**, *17*, 120–131. [CrossRef]
37. Hu, L.; Feng, P.; Meng, Y.; Yang, J. Buckling Behavior Analysis of Prestressed CFRP-Reinforced Steel Columns via FEM and ANN. *Eng. Struct.* **2021**, *245*, 112853. [CrossRef]
38. Tran, D.T.; Pham, T.M.; Hao, H.; Chen, W. Numerical Investigation of Flexural Behaviours of Precast Segmental Concrete Beams Internally Post-Tensioned with Unbonded FRP Tendons under Monotonic Loading. *Eng. Struct.* **2021**, *249*, 113341. [CrossRef]
39. Jiang, J.; Li, G.-Q. Progressive Collapse Analysis of 3D Steel Frames with Concrete Slabs Exposed to Localized Fire. *Eng. Struct.* **2017**, *149*, 21–34. [CrossRef]
40. Maj, M.; Ubysz, A. Cracked Reinforced Concrete Walls of Chimneys, Silos and Cooling Towers as Result of Using Formworks. *MATEC Web Conf.* **2018**, *146*, 02002. [CrossRef]
41. Safakhah, S.; Zahrai, S.M.; Kheyroddin, A. Using Two-Stage Method in Reinforced Concrete Bridge Piers for Damage Quantification. *Proc. Inst. Civ. Eng. Struct. Build.* **2019**, *172*, 422–436. [CrossRef]
42. Liu, S.-W.; Liu, Y.-P.; Chan, S.-L. Advanced Analysis of Hybrid Steel and Concrete Frames: Part 2: Refined Plastic Hinge and Advanced Analysis. *J. Constr. Steel Res.* **2012**, *70*, 337–349. [CrossRef]
43. Koukouselis, A.; Mistakidisa, E. Numerical Investigation of the Buckling Behavior of Thin Ferrocement Stiffened Plates. *Comput. Concr.* **2015**, *15*, 391–410. [CrossRef]
44. *SP 63.13330.2018*; Concrete and Reinforced Concrete Structures. General Provisions, Official Edition. Standartinform. Ministry of Construction and Housing and Communal Services of the Russian Federation: Moscow, Russia, 2019. Available online: https://docs.cntd.ru/document/554403082 (accessed on 15 February 2023).
45. Tamrazyan, A.; Alekseytsev, A.V. Optimization of reinforced concrete beams under local mechanical and corrosive damage. *Eng. Optim.* **2022**, 1–18. [CrossRef]
46. Alekseytsev, A.V. Mechanical safety of reinforced concrete frames under complex emergency actions. *Mag. Civ. Eng.* **2021**, *103*, 10306. [CrossRef]
47. Liu, D.; Wang, Z.; Pan, J.; Zheng, Y.; Hu, Z. Optimum Design of Nonlinear Semi-Rigid Steel Frame Based on Performance-Price Ratio via Genetic Algorithm. *J. Build. Eng.* **2022**, *61*, 105287. [CrossRef]
48. Alekseytsev, A.V.; Nadirov, S.H. Scheduling Optimization Using an Adapted Genetic Algorithm with Due Regard for Random Project Interruptions. *Buildings* **2022**, *12*, 2051. [CrossRef]